

## Asymmetry in the reciprocal epitaxy of NaCl and KBr

S. Maier,<sup>1,2</sup> O. Pfeiffer,<sup>1</sup> Th. Glatzel,<sup>1</sup> E. Meyer,<sup>1</sup> T. Filleter,<sup>2</sup> and R. Bennewitz<sup>2</sup>

<sup>1</sup>*Department of Physics and Astronomy, University of Basel, Basel, Switzerland*

<sup>2</sup>*Department of Physics, McGill University, Montreal, Quebec, Canada*

(Received 13 February 2007; published 4 May 2007)

Ultrathin well-ordered films of KBr on NaCl(100) and of NaCl on KBr(100) have been grown. The films were imaged by means of noncontact atomic force microscopy with atomic resolution under ultrahigh vacuum conditions. An extreme asymmetry in the structure of the interface was found for the two systems. The first layer of KBr on NaCl(100) grows with the lattice constant of bulk KBr, while the first layer of NaCl on KBr(100) stretches to the bulk lattice constant of KBr. The KBr films exhibit a superstructure with the periodicity of the least common multiple of the NaCl and KBr lattice constants, while the stretched NaCl films grow flat. We discuss the anharmonicity of the ionic bond as origin of the dependence of the interface structure on the growth sequence.

DOI: [10.1103/PhysRevB.75.195408](https://doi.org/10.1103/PhysRevB.75.195408)

PACS number(s): 68.55.Ac, 68.55.-a, 68.65.Cd, 68.37.Ps

### I. INTRODUCTION

The lattice mismatch in heteroepitaxy can result in large strain, whose relief creates a multitude of surface structures such as dislocation networks or periodic superstructures. These surface structures have interesting physical properties in themselves, but can also be used as templates for the heterogeneous nucleation of island superlattices, or for the regular arrangement of single molecules or molecular clusters.<sup>1</sup> A key for the understanding and prediction of the surface structures lies in an analysis of the microscopic structure of the interface between substrate and film. Heteroepitaxy of alkali-halide crystals provides model systems for studying strain relief structures on insulators because of the large range of lattice constants and the comparatively simple preparation. Heteroepitaxial growth for various combinations of alkali-halide crystals over a wide variety of lattice mismatches has been studied in a number of reflection high-energy electron diffraction (RHEED) experiments.<sup>2-5</sup> One important result is that alkali-halide thin films grow epitaxially in a layer-by-layer mode for lattice mismatches smaller than 20% and in a three-dimensional island mode for larger mismatches. Kiguchi *et al.*<sup>6</sup> analyzed that the lattice distortion in the film relaxed more rapidly for systems with a film lattice constant larger than the substrate lattice constant (positive misfit) as compared to systems with a smaller film lattice constant (negative misfit). The difference between the two cases was attributed to the anharmonicity of ionic bonds, which render the elongation of ionic bonds easier than their compression.

Scanning probe microscopy is not only the tool to reveal strain patterns and the underlying atomic structure in real space, it also allows us to study the development of individual islands at the very initial stage of film growth. The development of high-resolution noncontact atomic force microscopy (nc-AFM) has extended these capabilities towards insulating surfaces. Several scanning tunneling microscopy (STM) and nc-AFM studies have described the heteroepitaxial growth of ultrathin well-ordered alkali-halide films on metals and semiconductors.<sup>7-13</sup> For coverage of one or two atomic layers, a carpetlike growth mode was observed: The first layer grows in the form of large islands with hundreds of nanometers side length, smoothly covering substrate steps. The subsequent layers grow in the form of smaller rectangu-

lar islands with tens of nanometers side length. Very few atomic force microscopy studies have reported on the growth of alkali-halide films on alkali-halide crystals. Mazur *et al.* have described a layer-by-layer growth of 20 monolayers of LiBr on LiF(100) and the formation of rectangular pits in these films upon annealing as found in contact-mode AFM experiments.<sup>14</sup>

Theoretical models and numerical simulations propose various interface structures for the accommodation of the lattice mismatch at the interface of two alkali-halide crystals including stacking faults, elongated lattice constants, and surface rumpling.<sup>15-19</sup>

In the present study we characterize the submonolayer growth of films of KBr on NaCl(100) and of the complementary system NaCl on KBr(100) by means of nc-AFM in ultrahigh vacuum. NaCl and KBr have a lattice mismatch of 17%, the ratio of nearest-neighbor distances of NaCl and KBr is very close to 7:6. Despite the large lattice mismatch, a layer-by-layer growth has been observed in RHEED studies.<sup>5</sup> Duan *et al.*<sup>20</sup> found the signature of a superstructure on top of KBr films grown on NaCl(100) in helium atom scattering spectra. The periodicity of the superstructure was indeed 7 times the next-neighbor distance of the NaCl(100) surface. Here, we present images of the growth of the first layers of KBr and NaCl as observed in real space by force microscopy. Atomic resolution imaging allows us to describe an asymmetry in the interface structure, where a sharp step in the lattice constant which is accommodated by rumpling of several layers into a superstructure in the one system contrasts with a continuous transition of the lattice constant and a flat first layer in the other system.

### II. EXPERIMENTAL SETUP

All force microscopy measurements have been performed in ultrahigh vacuum (UHV) at room temperature using home-built atomic force microscopes operated in noncontact mode. Rectangular silicon cantilevers with integrated tips and a resonance frequency between 150–165 kHz were employed as force sensors. The silicon tips are covered with a thin native oxide layer since no particular tip treatment has been applied. For the noncontact mode experiments, the can-

tilver has been excited to oscillate at the first normal bending resonance with constant amplitude. The tip-sample distance was controlled by maintaining constant negative shift of the resonance frequency with respect to the resonance far from the surface.

Any occurrence of energy dissipation in the tip-sample interaction would damp the cantilever oscillation and require an increase of the excitation amplitude  $A_{\text{exc}}$  applied to the piezoactuator. Therefore,  $A_{\text{exc}}$  is often referred to as damping signal. Despite recent efforts, a quantitative understanding of  $A_{\text{exc}}$  measurements is not straightforward.<sup>21,22</sup> In this paper we exploit the characteristic distance dependence of the damping signal<sup>23</sup> to reveal surface structures with very small topographic corrugation. By recording the damping signal simultaneously with the topography signal, subtle details of the surface topography can be detected which are often lost by the feedback circuit working with the frequency shift signal, which is sensitive to long-ranged interactions.

Atomically flat and clean KBr(100) surfaces were prepared by cleaving a single crystal in air, followed by a quick transfer to the vacuum system and annealing in UHV at 120 °C for 30 minutes. The NaCl single crystals were cleaved in UHV and heated at 150 °C for 30 minutes in order to remove charges produced in the cleaving process. Previous to the evaporation, the cleaved surfaces were imaged by AFM to verify the cleanness and flatness of the surface. Ultrathin films of NaCl and KBr were evaporated on the clean substrate from a Knudsen cell. The evaporation rates were calibrated with a quartz microbalance and by analysis of the AFM images. Evaporation rates ranged from 0.1 Å/min to 2.4 Å/min.

### III. RESULTS

#### A. Heteroepitaxial growth of KBr on NaCl

The submonolayer growth of KBr on an atomically flat NaCl(100) surface is shown in Fig. 1(a). Rectangular islands with a height of two or three layers and a typical side length of 15 nm are homogeneously distributed over the surface. Islands of monolayer height are not observed. While the first two layers always form complete rectangular islands, the third layer may cover only part of the double-layer rectangular islands. The lateral size of islands depends on the evaporation rate: At higher evaporation rate islands with side length less than 15 nm are formed [compare Figs. 1(a) and 1(b)]. During evaporation the NaCl substrate was held at a temperature of 25 °C. A complete stripe of KBr decorates the upper terrace at an atomic step of the NaCl substrate. Some of the homogeneously distributed KBr islands on the lower terrace grow very close to the steps. However, none of the KBr islands are found to be overgrowing a substrate step.

The surface of the KBr islands exhibits a regular superstructure. This superstructure is observed on islands of both two-layer and three-layer height. The corrugation of the superstructure is too small compared to the island height to become visible in the topographic representation of the islands in Fig. 1(c). As described in Sec. II, the simultaneously recorded  $A_{\text{exc}}$  image in Fig. 1(d) reveals the superstructure clearly. The average signal on top of the islands is slightly

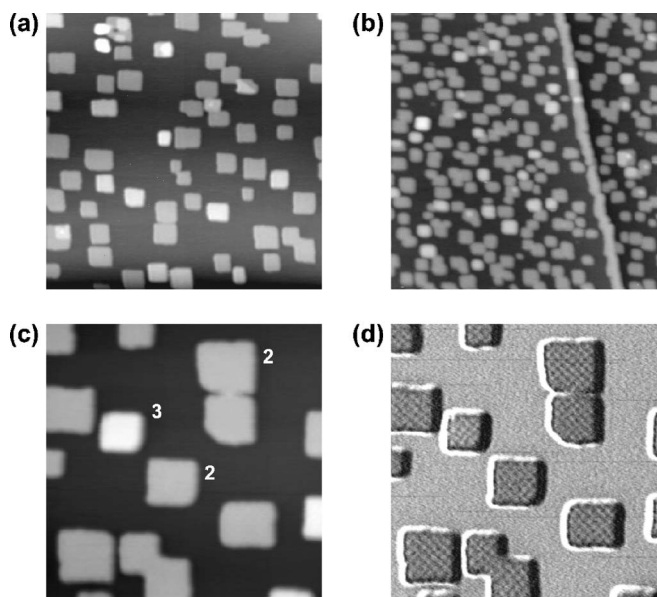


FIG. 1. (a)–(c) Topography and (d)  $A_{\text{exc}}$  images of a NaCl(100) surface partially covered with KBr. The typical size of the KBr islands with two and three layers height of 0.66 and 0.99 nm, respectively, depends on the evaporation rate: (a) slower rate of 0.1 Å/min and (b) higher rate of 2.4 Å/min. The topography image in (c) and the simultaneously recorded  $A_{\text{exc}}$  image in (d) show a detail of (a). Some islands with double-layer height and some of triple-layer height are labeled by numbers 2 and 3, respectively, in order to clarify the gray scale. Image sizes: (a) and (b) 200 nm  $\times$  200 nm; (c) and (d) 100 nm  $\times$  100 nm.

reduced compared to the substrate terrace due to a material contrast often found in  $A_{\text{exc}}$  images of heterogeneous surfaces.<sup>24</sup>

High-resolution images of small areas on top of a double-layer island are shown in Fig. 2. The periodicity of the superstructure is found to be  $3.97 \pm 0.05$  nm along the  $\langle 100 \rangle$  direction. The ratio of unit cell size in KBr and NaCl is nearly 6:7. Therefore, a periodicity of six unit cells of the KBr film, respectively, 3.96 nm could be expected for the periodicity of the superstructure. It is in agreement with the helium scattering results of Duan *et al.*<sup>20</sup> and the predictions of Baker *et al.*<sup>16</sup>

Figure 2 shows the topography (a) and the corresponding  $A_{\text{exc}}$  map (b) of the superstructure in detail, with a typical cross-section plotted in (c). The corrugation of the superstructure is observed to take values up to 0.12 nm on two-layer thick islands and up to 0.11 nm on three-layer thick islands. The measured corrugation increases towards the edge of islands, and depends strongly on the tip shape. These findings resemble the observations for corrugation variations in atomic resolution imaging of alkali-halide surfaces which were found to originate in the coordination of surface atom and in the details of the tip structure.<sup>25</sup>

The cross section of the damping signal in Fig. 2(c) shows an increased damping signal in the topographic valleys of the superstructure. This is the expected increase of the damping signal with decreasing distance of the macroscopic tip from the average surface position. The atomic lattice underlying the superstructure is revealed in high-resolution images in

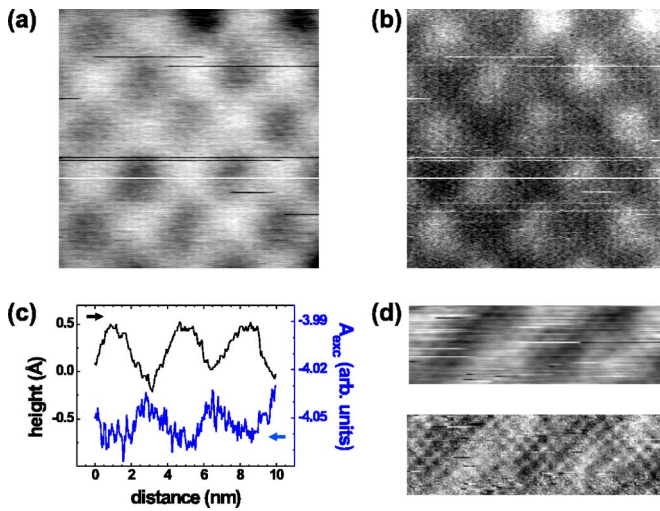


FIG. 2. (Color online) Topography (a) and  $A_{\text{exc}}$  map (b) showing the superstructure on top of a double layer KBr island grown on NaCl(100). The pronounced corrugation in the upper row of features can be attributed to the fact that this row forms the edge of the film. (c) Cross section of (a) and (b) along the white line. (d) Topography (upper image) and corresponding frequency shift image (lower image) showing atomic resolution across the superstructure. Image size: (a) and (b)  $10 \text{ nm} \times 10 \text{ nm}$ ; (d)  $10 \text{ nm} \times 3.1 \text{ nm}$ .

Fig. 2(d). The atomic periodicity appears pronounced in maps of the frequency shift in Fig. 2(d), i.e., of the error signal of the topographic feedback as the tip is moving quasi-at-constant height on the lateral scale of the atomic lattice. Fourier analysis of such images verifies a relation of 6:1 between the lattice constants of the superstructure and the KBr island surface.

In an attempt to grow a complete flat layer of the superstructure we have explored different growth rates and substrate temperatures. Evaporation of two full layers with a low rate of  $0.1 \text{ \AA}/\text{min}$  does not result in a completed second layer, see Fig. 3(a). The third monolayer continues to grow before the second monolayer is closed. In Fig. 3(b) one can clearly observe the superstructure on the second and the third layer while small patches of the open NaCl substrate appear flat. The same growth mode was observed for a higher evaporation rate, see Fig. 3(c).

In order to promote the formation of a closed layer of the superstructure we have grown KBr films at a slightly elevated substrate temperature. Figure 3(d) shows a film grown at the same conditions as the film shown in (a) except that the substrate was kept at  $90 \text{ }^\circ\text{C}$  during the evaporation. A similar density and size distribution of rectangular islands is found on a closed surface. These rectangular islands have monolayer height and are covered by an additional incomplete monolayer which exhibits irregular, dendritic shapes. Two interpretations of the result are possible: The closed surface below the rectangular islands is a complete double layer of KBr, the rectangular islands are part of the third layer comparable to the findings in (a) and the irregularly shaped layer is part of a fourth layer. Alternatively, the closed surface could be the NaCl substrate, and the islands part of the first and second layer of a reduced final coverage resulting from the elevated substrate temperature. The latter inter-

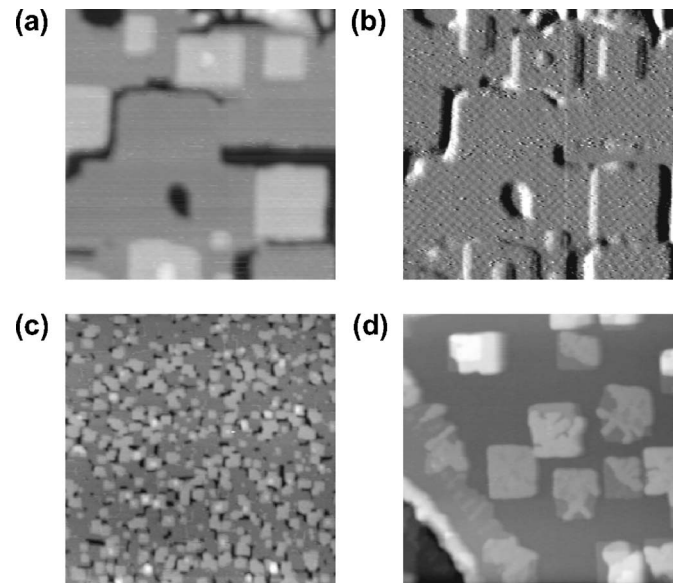


FIG. 3. Growth of approximately three layers of KBr on NaCl(100). Topography (a) and its derivative along the  $[100]$  direction (b) for an evaporation with a low rate of  $0.1 \text{ \AA}/\text{min}$  at room temperature ( $200 \text{ nm} \times 200 \text{ nm}$ ). The superstructure can be observed on the second and third layer while patches of the NaCl substrate appear flat. The evaporation with a high rate of  $1.8 \text{ \AA}/\text{min}$  in (c) looks similar to (a) ( $400 \text{ nm} \times 400 \text{ nm}$ ). In (d) the surface is shown after evaporation with a low rate of  $0.1 \text{ \AA}/\text{min}$  at a sample temperature of  $90 \text{ }^\circ\text{C}$  ( $300 \text{ nm} \times 300 \text{ nm}$ ). The rectangular islands are covered by an additional incomplete monolayer which exhibits dendritic shapes.

pretation seems supported by the fact that we could not observe the superstructure under these growth conditions. However, the calibration of the film thickness is not precise enough to decide between the two interpretations due to the unknown desorption rate at elevated temperatures.

For the growth of KBr films at elevated temperature one must consider the possibility of mixing of ionic species across the interface. Alkali-halide crystals are well known for forming solid solutions.<sup>26,27</sup> Such mixing adjusts the average lattice constant and may support the formation of monolayer islands and dendritic structures of KBr as observed here.

### B. Heteroepitaxial growth of NaCl on KBr

Figure 4(a) shows an overview image of the submonolayer growth of NaCl on a KBr(100) surface. The substrate was held at room temperature during the evaporation with the slower rate of  $0.1 \text{ \AA}/\text{min}$ . Rectangular islands are homogeneously distributed over the surface similarly to the growth of KBr onto NaCl(100). There is, however a significant difference in the growth mode between the two systems. The NaCl islands on KBr(100) have only monolayer height. Furthermore, their average size is larger at comparable evaporation rates.

The size of the islands decreases towards substrate steps. Figures 4(a) and 4(b) show how a series of smaller NaCl islands decorates the substrate steps on the upper terraces. On the lower terrace the NaCl islands are directly attached to



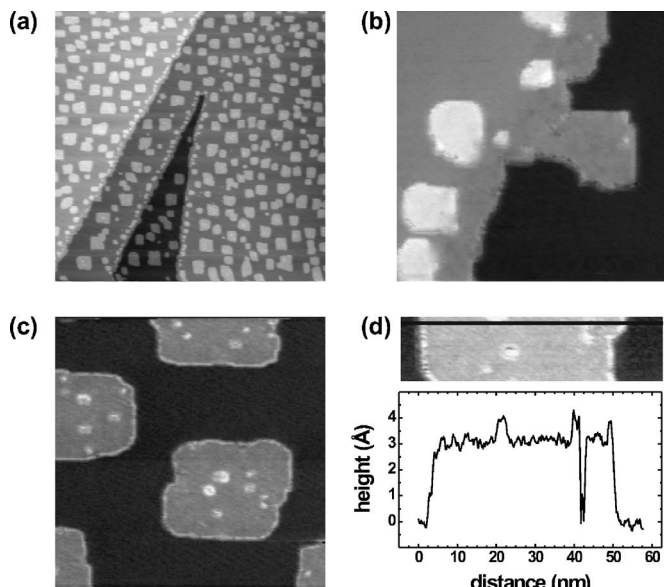


FIG. 4. Submonolayer growth of NaCl on KBr(100) at room temperature: NaCl islands of one monolayer height are homogeneously distributed on KBr(100) as illustrated in the overview image in (a) (1000 nm × 1000 nm). Frame (b) shows a NaCl island on a lower terrace which is directly attached to a KBr substrate step (80 nm × 80 nm). The detail image of the NaCl islands in (c) indicates that their edges contain several kinks and that on most islands a second layer starts growing (100 nm × 100 nm). In (d) the cross section of an island with a defect is shown.

the substrate steps. No clear transition between the attached NaCl islands and the upper terrace of the KBr substrate can be recognized in Fig. 4(b), not even in the atomic resolution image of the same area in Fig. 6(b). A complete stripe of NaCl seems to have grown along the substrate steps on the lower terrace. This conclusion is supported by the observation that the formerly straight substrate steps have an irregular appearance after evaporation of NaCl and by the finding that the series of smaller NaCl islands on the upper terrace has a distance of about 10 nm to the apparent substrate step.

A closer look into the NaCl islands reveals some growth irregularities, see Fig. 4(c). The island edges exhibit several kinks per island. On most islands a second layer starts to grow, and defects appear in some of the islands. A particular defect shown in the cross section in Fig. 4(d) turns out to be a hole with the depth of the island height. These irregularities may be the result of the large strain in the islands or from a coalescence of smaller precursor islands.

The rectangular shape of the islands described so far is the result of a minimization of corner and kink sites in the island edges and documents how energetically unfavorable corner and kink sites are for these systems. The situation changes for the NaCl island grown on KBr(100) at elevated temperature. Figure 5 shows the round shape of islands grown at a substrate temperature of 80 °C. The images demonstrate that at these growth temperatures a minimization of the length of the island edge becomes more favorable than a minimization of the number of kinks and corners.

The atomic structure of the monolayer NaCl islands on KBr(100) has been investigated in some detail. The structure

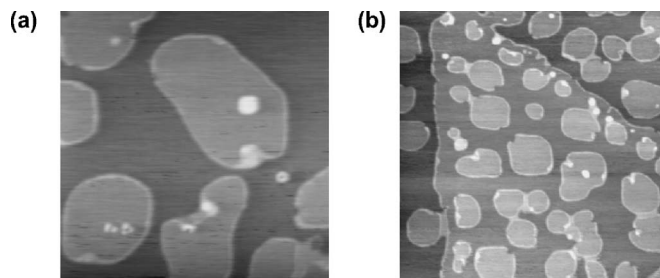


FIG. 5. The NaCl islands grown on KBr(100) at a substrate temperature of 80 °C exhibit a rounded shape. Frame sizes: (a) 200 nm × 200 nm and (b) 500 nm × 500 nm.

of both the substrate and an island are resolved in Fig. 6(a). The particular appearance of the step edge is a result of the convolution of the respective atomic structures of the tip apex and the step edge. While the immediate surrounding of the step is blurred by this effect, one can still recognize that the lattices of substrate and island have the same periodicity. A Fourier analysis confirms that the NaCl island and the surrounding KBr substrate have the same lattice constant, which is within an error identical to the lattice constant of the KBr(100) surface before growth of NaCl islands. We conclude that the ion-ion distance in the monolayer NaCl islands are enlarged to match the lattice of the KBr substrate. In agreement with this conclusion, no superstructure or dislocation network is observed on NaCl islands grown on KBr(100). The adaption of the KBr(100) lattice by the islands has been confirmed in many atomically resolved images. One example is the NaCl island attached to a KBr substrate step in Fig. 6(b).

With increasing thickness of the NaCl films we would expect the lattice constant to change towards the bulk lattice constant of NaCl. Figure 7(a) shows the KBr(100) surface after evaporation of approximately three layers of NaCl. The surface was held at room temperature during the evaporation and the rate was 0.1 Å/min. The surface appears rough compared to the complementary system discussed in Sec. III A.

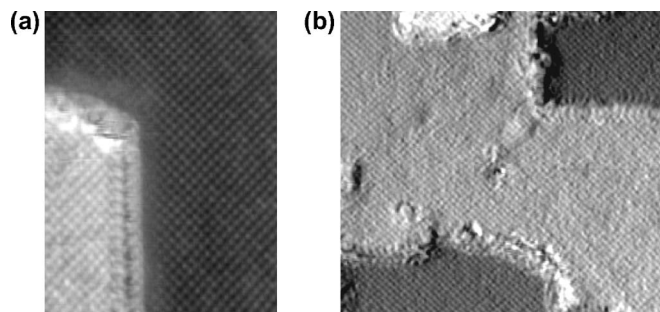


FIG. 6. (a) Atomic resolution images of both a NaCl island and the KBr substrate (15 nm × 19.6 nm). Note that the structure of the step edge results from the convolution of the atomic structures of tip apex and step edge. A Fourier analysis of such images confirms that the NaCl island and the KBr substrate have the same lattice constant. (b) Atomic resolution image of a NaCl island attached to a KBr substrate step (33 nm × 30 nm). The contrast of the atomic structure in both images has been amplified by adding the horizontal derivative of the topography to the original topography.

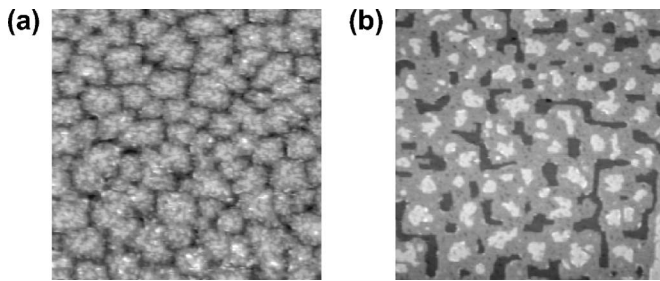


FIG. 7. Growth of approximately three layers of NaCl on KBr(100) at room temperature. The surface in (a) is rough compared to the complementary system shown in Fig. 3. (b) Annealing at temperatures increasing from 60 °C to 80 °C for 90 minutes results in a flatter surface with larger island size and less material in the third layer. Image sizes: 500 nm  $\times$  500 nm.

Annealing flattens the surface significantly. Figure 7(b) shows the same surface as in (a) after 90 minutes annealing at a temperature increasing from 60 °C to 80 °C. The first layer of NaCl seems now to be almost closed with only a few defects observed. Similar changes in topography upon annealing were observed for films of LiBr on KBr(100) and on LiF(100) by Goleck *et al.*<sup>28</sup> The authors attributed the changes to an Ostwald ripening which favors the growth of larger islands at the cost of smaller ones.

#### IV. DISCUSSION

The initial stage of the reciprocal heteroepitaxial growth of KBr and NaCl takes the form of rectangular islands of some tens of nanometer side length. Similar islands are observed in the growth of alkali-halide films on metals and semiconductors on top of the continuous first layer.<sup>7-12</sup> There are four significant differences between the case of positive misfit [KBr on NaCl(100)] and negative misfit [NaCl on KBr(100)]. For the positive misfit, the islands have a height of two or three atomic layers, the lattice constant of the islands is close to the bulk value of the island material, a superstructure is observed on the islands, and very few kinks and defects disturb the rectangular shape of the islands. For the negative misfit the initial island height is one monolayer, the lattice constant of the island takes the values of the underlying substrate, no superstructure is observed, and defects, kinks, and rounded edges impair the rectangular shape of the islands. The differences in the interface structure are schematically depicted in Fig. 8.

Our atomic-resolution microscopy results shed new light on previously reported diffraction experiments on similar growth systems. A helium scattering study of the positive misfit system KBr on NaCl(100) has reported the superstructure, the initial growth of a double layer, and the exposure of the NaCl substrate even after evaporation of three layers of KBr.<sup>20</sup> The very low intensity of the specular reflex in Duan's study for a coverage of two layers is explained by our real space data. The small size of the islands and the distribution of the island height between two and three layers height diminish coherent contributions to the specular scattering amplitude. The initial growth in the form of

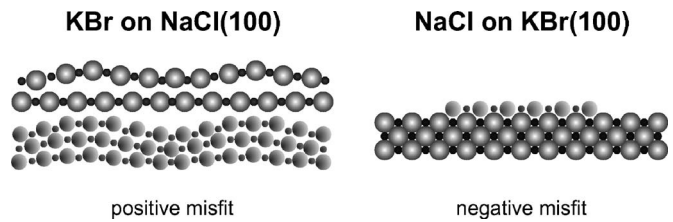


FIG. 8. Schematic representation of the results for the interface structure in the reciprocal epitaxy of KBr and NaCl. The indicated rumpling of the different layers in the case of positive misfit reflects the calculations by Baker and Lindgard (Ref. 16).

monolayer<sup>8</sup> or bilayer<sup>7,10</sup> islands is also known for the heteroepitaxy of alkali-halide films on metals and semiconductors. The lattice constant of films in heteroepitaxy approaches the bulk value of the film material for increasing films thickness. Kiguchi *et al.*<sup>6</sup> observed that the lattice distortion relaxes more rapidly for a positive misfit than for a negative misfit in the mutual heteroepitaxy of alkali-halide films. Our results for KBr and NaCl carry this tendency to an extreme. The positive misfit system grows from the first bilayer with its own bulk lattice constant, while the first layer in the negative misfit system adjusts perfectly to the underlying substrate. Kiguchi *et al.* explain the difference with the anharmonicity of the ionic bond which favors a stretching of the film in a negative misfit over a compression in the positive misfit. This concept seems to allow for a consistent interpretation of the results presented in this study.

Despite the relative simplicity of the ionic bond it is not a simple task to develop a model for the initial film growth in heteroepitaxy of alkali-halide films. A building block approach of dipolar molecules based on the attraction and repulsion of nearest-neighbor charges falls far short. As examples, Celli and Urzua have calculated that alkali-halide monomers adsorb with the cation on top of surface anions and are typically tilted around 45° against the vertical.<sup>29</sup> Baker and Lindgard have studied few layers of KBr on NaCl(100) and found that the corrugation of the superstructure is maximal for the top layer of the substrate, that the first layer of the film is hardly corrugated, and that the second and third layer again show a significant corrugation. Both groups stress the importance of next-nearest-neighbor interactions. Shluger *et al.* have studied heteroepitaxy of alkali-halide films with positive misfit and also found a buckling of islands.<sup>30</sup> With respect to the initial stages of film growth, these authors have pointed out the dependence of the misfit on cluster size.

The existence and periodicity of the superstructure observed in this study agree well with the predictions by Baker and Lindgard. It is worth noting that this prediction and our observation by force microscopy indicate a topographic modulation of the ions in the top layer. Superstructures in thin alkali-halide films observed by scanning tunneling microscopy rather point to a modulation of the electronic structure.<sup>31-33</sup> The corrugation of the superstructure measured in our force microscopy experiment is one order of magnitude higher than predicted by Baker and Lindgard and evaluated by Duan *et al.*<sup>20</sup> Such enhancement of corrugations is caused by the modulation of the short-range electrostatic

field and by a displacement of surface ions in the force field of the tip. Similar discrepancies between the corrugation predicted and measured by helium scattering on the one hand<sup>34</sup> and force microscopy on the other hand have also been described for the atomic corrugation of alkali-halide films and crystals.<sup>24,35</sup>

The island shapes observed in this study provide some insight into the growth mode and the dominating interactions. For the positive misfit system KBr on NaCl(100) the islands are compact double- or triple-layer squares with the KBr lattice constant and a few defects. The interaction between island molecules dominates over interactions with the substrate. The influence of the substrate shows up in the orientation of the islands and in the superstructure. There is enough diffusion in the growth process to allow for the formation of compact defect-free islands and an effective minimization of kink sites. Decreasing island size with increasing evaporation rate also indicates a homogeneous nucleation of the KBr islands. On the other side, the negative misfit system NaCl on KBr(100) is strongly influenced by the interaction between substrate and islands ions. The monolayer islands adapt the substrate lattice constant. A significant density of hole defects in the islands and of kinks in the island edges could indicate the effects of strain in the island or a limitation of diffusion of molecules in the growth process. It is tempting to speculate that the islands of the positive misfit systems grow from upright monomers with enhanced diffusion, while the negative misfit system grows from flat monomers with a diffusion limited by stronger interactions with the substrate. Such a view is partially supported by the calculations of Celli and Urzua mentioned above.<sup>29</sup>

The growth of the islands close to substrate steps is in agreement with the picture developed in the last paragraph. Step edges are preferred nucleation sites. In the case of positive misfit, a stripe of KBr with the width of a typical island decorates the step edge on the upper terrace, while square islands in homogeneous distribution grow on the lower terrace. In the case of negative misfit, a number of smaller islands similarly decorate the step edge on the upper terrace. However, the strong interaction of the NaCl with the substrate and the adaption of the substrate lattice constant enables the growth of a stripe of NaCl along the KBr step edge on the lower terrace.

Our attempts to extend the results on heteroepitaxial growth beyond the submonolayer range and to produce closed films with the features discussed above have met difficulties. For the positive misfit system a rather smooth growth up to two layers reflects the compactness of the initial island growth. However, gaps within the first double layer persist while the third layer starts to grow. Such gaps may be the result of the fact that the first isolated KBr islands are positioned relative to the underlying NaCl lattice. Their distance is not necessarily a multiple of the KBr lattice constant and, therefore, a smooth merger of two growing islands may be hindered. Furthermore, Shluger *et al.* have pointed out that the distortion of the substrate lattice extends beyond the adsorbate island. Such extended strain fields make gaps between islands energetically favorable.<sup>30</sup> The strain and the

defect density in the negative misfit system manifest themselves as significant roughness in the growth of three layers of NaCl on KBr(100). This rough film can be flattened to some extent by gentle annealing. However, the growth of NaCl on KBr(100) at an elevated temperature has revealed an intriguing phenomenon. The NaCl islands start to develop a round shape rather than minimize the number of edges in their steps by enhanced diffusion. Similarly surprising, the growth of KBr on NaCl(100) at an elevated temperature yields dendritic top layers on the KBr islands which do not exhibit the superstructure found at room temperature. The strain relaxation and the growth of such curved shapes at elevated temperature may be facilitated by the onset of mixing between the NaCl and KBr across the interface. Alkali-halide mixtures are known to form solid solutions. Spontaneous mixing of coevaporated species have been demonstrated<sup>26</sup> for room temperature as well as the incorporation of KBr from a molecular beam into a KCl(100) surface at elevated temperature.<sup>27</sup>

## V. CONCLUSION

We have explored the initial stages of the reciprocal epitaxial growth of NaCl and KBr in real space by means of noncontact atomic force microscopy. The positive misfit system KBr on NaCl(100) grows in compact rectangular islands of double and triple layer height with the bulk lattice constant of KBr. The misfit between the KBr islands and the substrate gives rise to a superstructure that can be clearly resolved by force microscopy. The initial growth is very different for the negative misfit system NaCl on KBr(100). The NaCl islands exhibit monolayer height and adapt the lattice constant of the underlying lattice. The strain gives rise to defects and kinks and causes a roughness in the growth of subsequent layers. The difference in the growth of the two systems can be understood in terms of the anharmonicity of the ionic bond which enables the elongation of bonds for the negative misfit case but produces a superstructure with the periodicity of the least common multiple of the lattice constants in the positive misfit case. The high resolution capability of force microscopy allows for a direct examination of the atomic structure of the interface in epitaxy, which plays a crucial role for the quality of epitaxial films. For the interface between KBr and NaCl two extremes can be stabilized, a jump of the lattice constant directly at the interface accommodated by rumpling into a superstructure and a stretching of the first NaCl layer to adapt the lattice constant of KBr. The example illustrates the dependence of epitaxial structures on the actual growth process as introduced by the anharmonicity of bonds.

## ACKNOWLEDGMENTS

The authors gratefully acknowledge fruitful discussions with Alexis Baratoff. This work was supported by the Canada Foundation of Innovation, the NSERC, the Swiss National Science Foundation and the Swiss NCCR on Nanoscale Science.



- <sup>1</sup>H. Brune, *Single Molecules at Surfaces* (Springer, New York, 2006), Chap. Supperlattices of atoms, molecules, and islands.
- <sup>2</sup>L. G. Schultz, *Acta Crystallogr.* **5**, 130 (1952).
- <sup>3</sup>M. H. Yang and C. P. Flynn, *Phys. Rev. Lett.* **62**, 2476 (1989).
- <sup>4</sup>M. H. Yang and C. P. Flynn, *Phys. Rev. B* **41**, 8500 (1990).
- <sup>5</sup>K. Saiki, *Appl. Surf. Sci.* **133/114**, 9 (1997).
- <sup>6</sup>M. Kiguchi, K. Saiki, and A. Koma, *Surf. Sci.* **470**, 81 (2000).
- <sup>7</sup>K. Glöckler, M. Sokolowski, A. Soukopp, and E. Umbach, *Phys. Rev. B* **54**, 7705 (1996).
- <sup>8</sup>W. Hebenstreit, J. Redinger, Z. Horozova, M. Schmid, R. Podloucky, and P. Varga, *Surf. Sci.* **424**, L321 (1999).
- <sup>9</sup>R. Bennowitz, M. Bammerlin, M. Guggisberg, C. Loppacher, A. Baratoff, E. Meyer, and H.-J. Güntherodt, *Surf. Interface Anal.* **27**, 462 (1999).
- <sup>10</sup>J. Repp, G. Meyer, and K.-H. Rieder, *Phys. Rev. Lett.* **92**, 036803 (2004).
- <sup>11</sup>J. Repp, S. Fölsch, G. Meyer, and K.-H. Rieder, *Phys. Rev. Lett.* **86**, 252 (2001).
- <sup>12</sup>S. Fölsch, A. Riemann, J. Repp, G. Meyer, and K.-H. Rieder, *Phys. Rev. B* **66**, 161409(R) (2002).
- <sup>13</sup>J. Kolodziej, B. Such, P. Czuba, F. Krok, P. Piatkowski, and M. Szymanski, *Surf. Sci.* **506**, 12 (2002).
- <sup>14</sup>P. Mazur and F. Golek, *Phys. Status Solidi A* **202**, R155 (2005).
- <sup>15</sup>M. Henzler, C. Homann, U. Malaske, and J. Wollschläger, *Phys. Rev. B* **52**, R17060 (1994).
- <sup>16</sup>J. Baker and P. A. Lindgard, *Phys. Rev. B* **54**, R11137 (1996).
- <sup>17</sup>J. Baker and P. A. Lindgard, *Phys. Rev. B* **60**, 16941 (1999).
- <sup>18</sup>A. Natori, A. Tanaka, and H. Yasunaga, *Thin Solid Films* **281-282**, 39 (1996).
- <sup>19</sup>A. Natori, K. Toda, A. Tanaka, and H. Yasunaga, *Appl. Surf. Sci.* **130-132**, 616 (1998).
- <sup>20</sup>J. Duan, G. Bishop, E. Gillman, G. Chern, S. Safron, and J. Skofronick, *Surf. Sci.* **272**, 220 (1992).
- <sup>21</sup>M. Gauthier and M. Tsukada, *Phys. Rev. Lett.* **85**, 5348 (2000).
- <sup>22</sup>L. Kantorovich, *J. Phys.: Condens. Matter* **13**, 945 (2001).
- <sup>23</sup>C. Loppacher, R. Bennowitz, O. Pfeiffer, M. Guggisberg, M. Bammerlin, S. Schär, V. Barwich, A. Baratoff, and E. Meyer, *Phys. Rev. B* **62**, 13674 (2000).
- <sup>24</sup>R. Bennowitz, A. S. Foster, L. N. Kantorovich, M. Bammerlin, C. Loppacher, S. Schär, M. Guggisberg, E. Meyer, and A. L. Shluger, *Phys. Rev. B* **62**, 2074 (2000).
- <sup>25</sup>R. Bennowitz, S. Schaer, E. Gnecco, O. Pfeiffer, M. Bammerlin, and E. Meyer, *Appl. Phys. A: Mater. Sci. Process.* **78**, 837 (2004).
- <sup>26</sup>Y. Kimura, Y. Saito, T. Nakada, and C. Kaito, *Physica E (Amsterdam)* **13**, 11 (2002).
- <sup>27</sup>H. Dabringhaus and M. Haag, *Surf. Sci.* **281**, 133 (1993).
- <sup>28</sup>F. Goleck, P. Mazur, Z. Ryska, and S. Zuber, *Surf. Sci.* **600**, 1689 (2006).
- <sup>29</sup>V. Celli and G. Urzua, *J. Phys.: Condens. Matter* **5**, B91 (1993).
- <sup>30</sup>A. L. Shluger, A. L. Rohl, and D. H. Gay, *Phys. Rev. B* **51**, 13631 (1995).
- <sup>31</sup>K. Kobayashi, *Phys. Rev. B* **53**, 11091 (1996).
- <sup>32</sup>J. Repp, G. Meyer, F. Olsson, and M. Persson, *Science* **305**, 493 (2004).
- <sup>33</sup>M. Pivetta, F. Patthey, M. Stengel, A. Baldereschi, and W.-D. Schneider, *Phys. Rev. B* **72**, 115404 (2005).
- <sup>34</sup>G. Chern, J. G. Skofronick, W. P. Brug, and S. A. Safron, *Phys. Rev. B* **39**, 12828 (1989).
- <sup>35</sup>R. Bennowitz, O. Pfeiffer, S. Schär, V. Barwich, and E. Meyer, *Appl. Surf. Sci.* **188**, 232 (2002).